Thermodynamics of Pure Dipolar Fluids. 1. The Water and Ammonia Cases

Ana Laura Benavides* and Yolanda Guevara

Instituto de Física, Universidad de Guanajuato, Apdo. Postal E-143, León Gto., México

Received: October 28, 2002; In Final Form: June 13, 2003

A molecular-based equation of state derived from perturbation theory is used to study the phase diagram and thermodynamic properties of water and ammonia in the fluid phase region. The molecular model that represents these substances consists of spherical particles interacting via a square-well potential with an embedded point dipole. The equation of state is an analytical expression, which depends explicitly on density, on temperature, and on the four adjustable parameters of the potential model: the particle's diameter, the energy depth and range of the square-well interaction, and the dipolar moment strength. Although the associating behavior due to hydrogen bonding that characterizes water and ammonia is not modeled by the perturbation approach followed in this paper, the theory is able to predict (except in the critical region) the vapor−liquid phase diagram and the saturation pressures, with accuracy close to that of theories that include a modeling of the H-bonding effects. A detailed comparison of experimental data from our theory and from three different approaches based on the Wertheim perturbation theory for associating fluids is presented. This comparison indicates that none of the later theories is able to give an accurate prediction within experimental error of the phase diagram of water, for the whole region of densities and temperatures for the fluid phase. This paper presents the ranges of values for density and temperature where each theory is accurate. Since the theory presented gives comparable predictions to those of the other equations, the dipolar square-well potential used in this work could be considered a good effective potential for associating polar fluids if the dipolar moment of the substance is taken slightly higher than its real value, an indication that by increasing the dipolar moment strength it is possible to mimic, at least in relation to thermodynamic properties, the H-bonding effects. The simplicity of this model can be useful as an important ingredient in the building of better equations of state for polar associating fluids.

1. Introduction

Water is the most important compound for biological systems and for many industrial processes, and yet it is the least understood substance.[1] It exhibits an anomalous behavior in several of its thermodynamic properties compared to most substances. Different potential models have been proposed to describe the thermodynamics of water, by using either simulation techniques or molecular-based theories, but up to now there has been no potential model that can accurately describe the entire phase diagram for this substance.[2−17] Since water is a polar substance and forms hydrogen bonds, both features must be included in a complete model for this substance, and the same conclusion is valid for ammonia.

Perturbation theory has been proved to be a reliable method to predict the thermodynamic properties of families of substances with similar molecular features. To study the behavior of fluids of molecules having permanent multipolar moments, a multipolar square-well perturbation theory (MSWPT)[18,19] has been developed. This theory provides a theoretical equation of state for a fluid formed by spherical particles interacting via a binary potential that considers overlap, dispersion, and electrostatic interactions. This theory has been applied to model the phase diagram of real polar substances with a permanent linear quadrupole moment[20] or an octopole moment.[21] Very good results are obtained when compared with experimental data. The theory can also predict accurately the speed of sound of several substances, as it has been discussed elsewhere. For the class of substances that have a permanent dipole moment, the MSWPT reduces to the case of the theory for a dipolar square-well fluid.

In this work we present an application of the MSWPT approach using the equation of state derived from this theory (DSWTEOS) to polar associating substances such as water (H_2O) and ammonia (NH_3). We will focus our attention on the use of the DSWTEOS to predict thermodynamic properties and the phase diagram. Although these substances form hydrogen bonds and consequently behave as associating fluids, an effect not considered explicitly by the DSWTEOS, we wanted to assess the predictions obtained by this theory when compared to those of more complex approaches that model the hydrogen-bonding effects explicitly, like the SAFT-VR[22] and SAFT-DY[23] approaches, as well as the Nezbeda and Weingerl equation of state (NW).[24] For the case of water, we will show that the DSWTEOS predictions are comparable to the results obtained using the theories already mentioned, if we consider a dipolar moment strength higher than the real value. This result suggests that the dipolar square-well model can be used as an effective intermolecular potential for polar substances, even if they are associating fluids, by increasing the dipolar moment strength. However, we will also show that all these molecular-based equations can only give, within experimental accuracy, partial predictions of the fluid phase diagram of water and we still lack a theory that can give an accurate prediction of the full fluid region of the phase diagram. This work emphasizes the relevance of a simple effective potential model for polar systems, which can also be easily implemented in any approach based on the Wertheim perturbation theory for associating fluids, such as SAFT. This can offer a more detailed model for water molecules and other

* To whom correspondence should be addressed. E-mail: alb@fisica.ugto.mx. Fax (52 477) 7885100.

10.1021/jp0223197 CCC: $25.00
Published on Web 07/26/2003

associating polar substances, providing analytical equations of state with an explicit dependence on the potential parameters for the dispersion interaction, dipolar moment, and hydrogen-bonding potential parameter. For instance, Liu et al.[23] considered for the SAFT-DY equation a dipolar Yukawa potential with and without the association term originated by the hydrogen bonds, using a Yukawa potential of fixed range ($\lambda = 1.8$). They found that including the association term for water and for ammonia improved their results, as expected. A similar approach can be followed for a dipolar square-well model of variable range, instead of the dipolar Yukawa potential of fixed range, on the basis of the equivalence between a SW and a Yukawa fluid of variable range.[25]

In section 2 the DSWTEOS is discussed, and in section 3 we present its application to predict the vapor−liquid phase diagrams for water and ammonia, including also a comparison with other theories. A test for the predictive capability in single phases is analyzed in section 4, where the pressures and isochoric heat capacities obtained are compared with available experimental data. Finally, in section 5 the main conclusions and perspectives of this work are presented.

2. Multipolar Square-Well Perturbation Theory

The DSWTEOS is based on the multipolar square-well perturbation theory,[1] which considers a system of spherical particles interacting via a square-well potential of variable range plus a dipole−dipole interaction in order to describe a binary effective intermolecular potential that takes into account overlap, dispersion, and electrostatic forces. The square-well potential (u_{SW}) is described by three parameters, a diameter σ, a depth ϵ, and a range λ, and is given by

$$u_{SW}(r_{12}) = \begin{cases} \infty & r_{12} \le \sigma \\ -\epsilon & \sigma < r_{12} \le \lambda\sigma \\ 0 & r_{12} > \lambda\sigma \end{cases} \quad (1)$$

where r_{12} is the center-of-mass to center-of-mass intermolecular distance.

The dipole−dipole interaction for a pair of charge distributions with identical dipole moment μ is given in terms of the orientations of each charge distribution, $\Omega_1 = (\theta_1, \phi_1)$ and $\Omega_2 = (\theta_2, \phi_2)$, where θ_i and ϕ_i are the polar and azimuthal angles for the point-dipolar moment vector with respect to r_{12}.

$$u_{DD} = \left(\frac{-\mu^2}{r_{12}^3}\right)(2\cos\theta_1\cos\theta_2 - \sin\theta_1\sin\theta_2\cos(\phi_1 - \phi_2)) \quad (2)$$

On the basis of the Barker and Henderson high-temperature perturbation expansion, the reduced Helmholtz free energy $a = A/NkT$ for a dipolar square-well fluid of N particles contained within a volume V and at temperature T can be written as the sum of two terms:[1]

$$a_{DSW}(T^*,\rho^*,\lambda,\mu^*) = a_{SW}(T^*,\rho^*,\lambda) + a_D(T^*,\rho^*,\mu^*) \quad (3)$$

Both contributions to the free energy are expressed as a function of the following reduced variables: $T^* = kT/\epsilon$, $\rho^* = (N/V)\sigma^3$, and $\mu^* = (\mu^2/\epsilon\sigma^3)^{1/2}$, with k as Boltzmann's constant. The first term, a_{SW}, is the Helmholtz free energy due to overlap and dispersion forces, as modeled by a square-well fluid of variable range, and the second term, a_D, gives the dipolar contribution to the free energy. According to the perturbation theory, there are also contributions to the free energy originated by crossed SW-dipolar terms that are neglected in the DSW-TEOS, since they appear as third-order terms in the perturbation expansion. Therefore, the DSWTEOS only requires square-well and dipolar equations of state. Several equations of state are available for the square-well fluid,[26−29] and for our research we used the analytical equation of state (SWTEOS) proposed by Gil-Villegas et al.,[29] obtained by perturbation theory. This equation is accurate enough over the whole fluid range, with the exception of the critical region, and for SW systems with ranges $1.25 \le \lambda \le 2$.

The MSWPT uses as a reference system the hard-spheres fluid, and the dipolar contribution to the free energy a_D is the Larsen *et al.*[30] expression, derived from a Padé approximation. The DSWTEOS is described in the Appendix. The DSWTEOS is an analytical equation in the critical point and, consequently, fails to predict accurately the critical region.[31]

TABLE 1: Optimized Intermolecular Potential Parameters for Water and Ammonia for the Dipolar Square-Well Theoretical Equation of State (DSWTEOS)[a]

substance	σ/nm	(ϵ/k)/K	λ	μ^*
H_2O	0.2996	407.585	1.4	1.75
NH_3	0.3223	201.47	1.5	2.00

[a] The parameters are the diameter σ, the depth ϵ/k, and the range λ of the square-well potential, and $\mu^* = \{\mu^2/(\epsilon\sigma^3)\}^{1/2}$ is the reduced dipole moment strength.

TABLE 2: Dipole Moment Strength μ for Water and Ammonia[a]

substance	μ(DSWTEOS)/10^{-18} esu	μ(ref 33)/10^{-18} esu
H_2O	2.15	1.855, 1.875, 2.00
NH_3	1.93	1.47, 1.51, 1.61

[a] The predictions of the DSWTEOS are shown in the second column as absolute values, and in the third column some reported values are presented.[33]

3. Results

To apply this theory to real fluids, we focused our attention on the vapor−liquid phase diagram and on the thermodynamic properties: pressure (P) and isochoric heat capacity (C_V) in the vapor, liquid, and supercritical regions. The four potential-model parameters σ, ϵ, λ, and μ^* were optimized by fitting the saturated liquid densities and the saturated vapor pressure curves to experimental data obtained from the NIST tables[32] for both substances. The optimized parameters for the DSWTEOS are given in Table 1.

By knowing the values of μ^*, σ, and ϵ/k, it is then possible to calculate the corresponding dipole moment strength (μ) for each substance in esu units, since $\mu^* = (\mu^2/\epsilon\sigma^3)^{1/2}$. When compared with experimental values[33] (Table 2), it is observed that, although the predicted values are of the same order of magnitude as the experimental values, they are systematically higher than the real dipolar moment strengths (approximately 13% for water and 26% for ammonia, taking the average values of the experimental data as reference). These results indicate that the theory is able to reproduce the behavior of polar associating substances without an explicit contribution to the free energy due to H-bonding, just by increasing the value of the dipolar moment strength. Although this seems to be a rather artificial procedure, the suggested effect observed here is that the thermodynamic effect arising from the H-bonding contribution can also be represented by a stronger dipolar contribution.

Water. The vapor−liquid phase diagram of water is shown in Figure 1. The DSWTEOS prediction is compared with the NIST data.[32] The general shape of the orthobaric curve fits

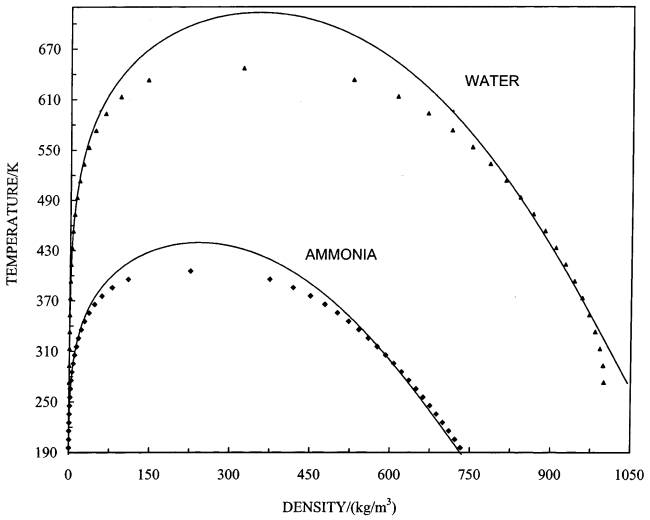

Figure 1. Coexistence curves for water and ammonia. The continuous line corresponds to the DSWTEOS; the ◆ and the ▲ are the experimental data for ammonia and water, respectively, from the NIST tables.[32]

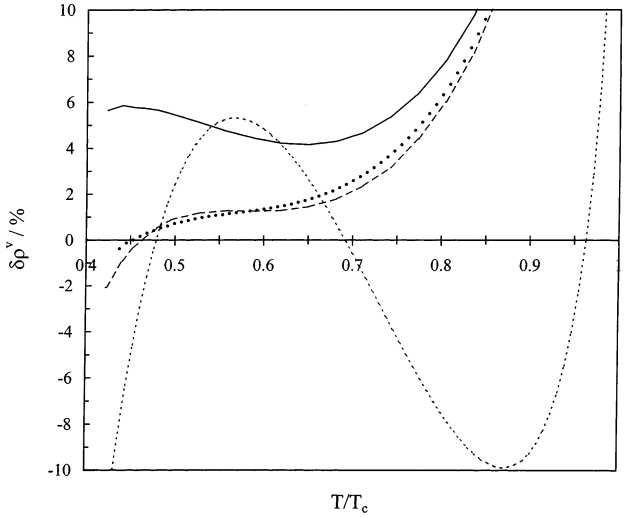

Figure 2. Percentage deviations in the vapor saturated densities $\delta\rho^V$ of the theoretical predictions with respect to the experimental data for water. The interpolation continuous curves correspond to the DSWTEOS, the long-dashed curves to the SAFT-VR, the dotted curve to the SAFT-DY, and the dashed curves to the NW.

qualitatively well with the experimental data. As expected, the critical region is not well predicted. Near the triple point, the liquid saturated densities are overestimated, but in this zone there is evidence that a fluid−fluid transition[35] may be present and that more detailed experimental data and theoretical approaches are required.

To see the accuracy of the predicted saturated densities, we present in Figures 2 and 3 deviation plots that indicate the percentage deviations in the orthobaric density $\delta\rho = 100(\rho^{exp} - \rho^{theo})/\rho^{exp}$ against T/T_c, for vapor and liquid, respectively. For the experimental data we used the Kruse and Wagner parametrization.[34] The temperatures spanned the range from the triple point $T_t = 273.163$ K to the critical point $T_c = 647.096$ K.[34] We have included the SAFT-VR, the SAFT-DY, and the NW deviations.

In Figure 4 the saturated pressure predictions of the DSWTEOS are presented, obtaining a very good representation with the exception of the critical point. As predicted, this point is overestimated. In Figure 5 the percentage deviations in the

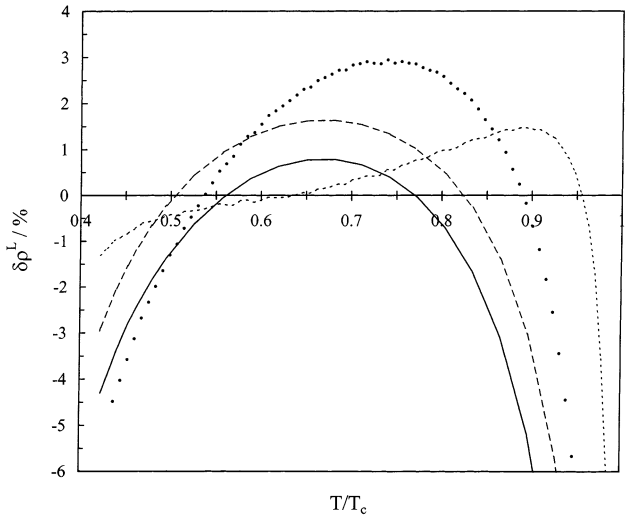

Figure 3. Percentage deviations in the liquid saturated densities $\delta\rho^L$ of the theoretical predictions with respect to the experimental data for water. See Figure 2 for details.

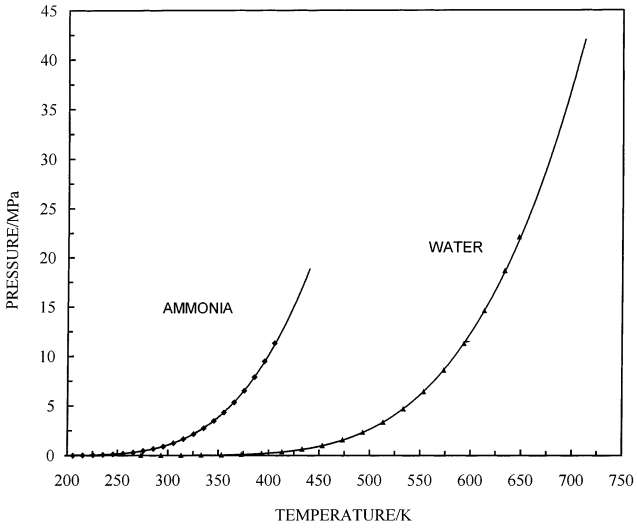

Figure 4. Saturated vapor pressures as a function of the temperature for water and ammonia. See Figure 1 for details.

saturated pressures, $\delta P = 100\%(P^{exp} - P^{theo})/P^{exp}$, are given as a functions of T/T_c. The best predictions come from the SAFT-type equations followed by the DSWTEOS, whereas the NW predictions have the largest deviations.

In Table 3 the overall performance of all the equations considered is summarized. We present the average absolute deviations (AADs) and the maximum deviation for the coexistence densities, ρ^V and ρ^L, and for the saturated pressure P for temperatures between 283.15 and 643.15 K. The generated data for all the equations had an increment of temperature of 5 K. As can be seen, the NW equation gives the best predictions for the coexistence densities, followed by the SAFT-type equations and the DSWTEOS. For the saturated pressure the SAFT-DY gives the best prediction followed by SAFT-VR and the DSWTEOS. For this property the NW equation presents the larger deviations.

A further analysis that could be useful for an experimentalist is shown in Table 4. In this table we present a comparison of the overall performance up to 1% in the saturated properties of the different equations considered in this work from the triple to the critical points. The intervals of temperature and the percentage of the region of the vapor−liquid phase diagram

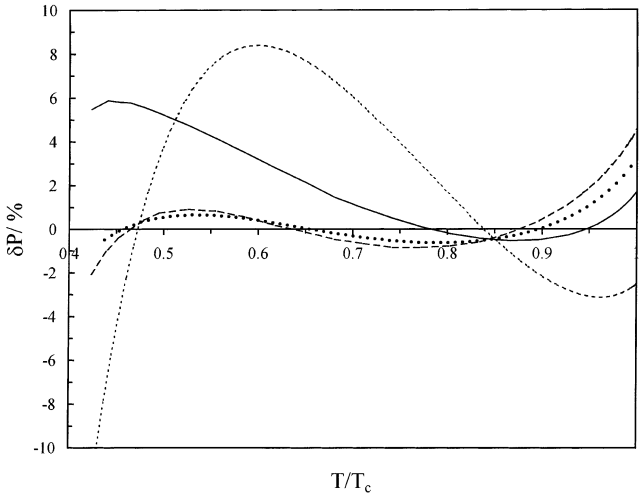

Figure 5. Percentage deviations in the saturated pressures δP of the theoretical predictions from the experimental data for water. See Figure 2 for details.

TABLE 3: Comparison of the Overall Performance of the DSWTEOS (Average Absolute Deviation (AAD) and Maximum Deviation) with Commonly Used Equations in the Interval 283.15−643.15 K

	AAD (%)			max. dev (%)		
equation	ρ^V	ρ^L	P	$\rho^{V_{max}}$	$\rho^{L_{max}}$	P^{max}
DSWTEOS	10.3	3.7	2.0	49.7	40.1	5.7
NW	5.3	0.9	4.3	20.3	12.7	8.3
SAFT-VR	7.8	3.0	0.8	48.7	33.0	4.1
SAFT-DY	7.7	3.1	0.5	48.5	30.1	2.8

TABLE 4: Comparison of the Overall Performance of the Different Equations of State Considered in This Work up to 1% in the Saturated Properties from the Triple to Critical Points

equation of state	interval[a]/K		
	ρ^V	ρ^L	P
DSWTEOS	0%	[333.15, 523.15] 51%	[458.15, 633.15] 47%
NW	[308.15, 318.18], [438.15, 453.16] and [623.15, 625.42] 7%	[283.17, 523.18] and [608.14, 623.15] 68%	[303.16, 308.15] and [528.16, 558.12] 9%
SAFT-VR	[288.15, 323.15] 9%	[303.15, 358.15] and [503.15, 553.15] 28%	[288.15−593.15] 82%
SAFT-DY	[283.15, 343.15] 16%	[333.15, 368.15] and [563.15, 583.15] 15%	[283.15, 612.80] 88%

[a] Below the intervals of temperature the percentage of the region of the liquid−vapor phase diagram that is reproduced within this error is included.

that is reproduced within this error are presented. The saturated vapor densities are reproduced within this error only in a very small region by all the equations considered, and the best predictions come from the SAFT-DY equation. The DSWTEOS does not reproduce this property within this error. For the saturated liquid densities the NW equation and the DSWTEOS equation cover a considerable greater region than the SAFT-VR and SAFT-DY equations. For the saturated pressures the SAFT-DY and SAFT-VR almost cover the full saturation curve, followed by the DSWTEOS (that covers almost half of this curve), while the NW equation reproduces only 9% of it. We can conclude that all the equations considered here cannot predict the entire phase diagram region and they have different performances in different regions of density and temperature. Also, different equations have different capabilities to reproduce simultaneously the liquid−vapor densities and the saturated pressures, a requirement that is very often desirable for industrial applications. However, the main conclusion derived from our work is that the DSWTEOS has, overall, a similar performance to those of the three associating theories compared here. An additional feature of this theory is that it can easily be extended to mixtures. For industrial purposes, sometimes in the absence of accurate equations of state for complex fluids, an approach like the one behind the DSWTEOS can be useful. Our approach indicates how the explicit dependence on the dipolar moment strength in the equation of state can be used to reproduce the same thermodynamic effects that the associating theories are able to model. A full study about the possibility of using a nonassociating polar fluid model to represent a true associating polar fluid substance, by adjusting the dipolar strength moment, following some sort of corresponding states principle, can be considered in the future, and this paper is a first attempt in this direction.

Finally, the experimental and theoretical pressure and the isochoric heat capacity for different phase states (vapor, supercritical, and liquid) for water are presented in Table 5, as functions of temperature and density, as obtained from the DSWTEOS. The percentage deviations in the pressure δP and the percentage deviations in the isochoric heat capacity at constant volume $\delta C_V = 100\%(C_V^{exp} - C_V^{DSWTEOS})/C_V^{exp}$ are also included. As can be seen, the pressure predictions for the states in the vapor phase are very good and the average of the absolute values of the deviations is 1.2%, while, for the supercritical states, the average is 3%. For the C_V in the vapor region, the average deviation is 8%, and for the supercritical states, this average is 6.7%. The liquid states show larger deviations for both properties; the average deviations are around 27%. Similar results are obtained with the SAFT-VR approach.

Ammonia. The vapor−liquid phase diagram of ammonia is shown in Figure 1. The DSWTEOS is compared with the NIST data.[32] The DSWTEOS reproduces the phase diagram except near the critical point, and it deviates slightly from the experimental data in the liquid branch.

In Figure 6, a deviation plot shows $\delta\rho$ against T/T_c, covering from the triple point $T_t = 195.49$ to the critical point $T_c = 405.4$ K. The DSWTEOS absolute average deviation (AAD) for the saturated vapor densities is 6%, and that for the saturated liquid densities is 1.2%, for the region $0.48 < T/T_c < 0.90$. The SAFT-DY predicts for $0.52 < T/T_c < 0.99$ the AAD of 2.9% and 1.33% for the saturated vapor and liquid densities, respectively. Since the regions of temperature considered for both equations are different, one can only say that the performances of both equations are comparable; in both regions the worst performance of the equation concerning the saturated vapor predictions is not considered. In Figure 4, the saturated pressure predictions are plotted as a function of temperature. The agreement with the experimental data for the DSWTEOS is good except that it overestimates the critical pressure. In Figure 7, δP is shown as a function of T/T_c. The absolute average deviations of the DSWTEOS are 0.75% for the entire analyzed region (from the triple to the critical points). The AAD of the SAFT-DY equation for $0.52 < T/T_c < 0.99$ is 2.3%. For this property the DSWTEOS has better predictions than SAFT-DY.

In Table 6, the experimental and theoretical pressures and isochoric heat capacities in the vapor, supercritical, and liquid phases for ammonia are presented for a wide range of temper-

TABLE 5: Experimental and Theoretical Pressures and Isochoric Heat Capacities for Water in the Vapor (V), Liquid (L), and Supercritical (Sc) Phases[a]

T/K	ρ/(kg/m^3)	P^{exp}/MPa	$P^{DSWTEOS}$/MPa	δP/%	C_V^{exp}/(kJ/(kg K))	$C_V^{DSWTEOS}$/(kJ/(kg K))	δC_V/%	phase
300	0.0256	0.004	0.004	0.0	1.44	1.40	2.8	V
350	0.006	0.001	0.001	0.0	1.42	1.41	0.7	V
400	1.3694	0.246	0.249	1.2	1.64	1.45	11.6	V
475	4.830	1.000	1.023	2.3	1.74	1.51	13.2	V
500	3.5909	0.8	0.81	1.2	1.63	1.51	7.4	V
525	4.279	1.0	1.01	1.0	1.63	1.53	6.1	V
525	8.925	2.0	2.06	3.0	1.80	1.55	13.9	V
800	14.017	5.00	5.04	0.8	1.76	1.71	2.8	Sc
800	29.107	10.00	10.19	1.9	1.84	1.74	5.4	Sc
800	482.23	100.00	107.20	7.2	2.62	2.13	18.7	Sc
850	70.594	24	24.98	4.1	2.01	1.83	8.95	Sc
900	58.619	22.06	22.73	3.0	1.95	1.84	5.6	Sc
1000	22.241	10.00	10.10	1.0	1.88	1.85	1.6	Sc
1000	60.378	26.00	26.72	2.8	1.97	1.89	4.1	Sc
350	978.09	10.00	6.07	39.3	3.87	2.34	39.5	L
350	982.39	20.00	29.17	45.9	3.85	2.34	39.2	L
500	831.65	3.00	2.19	27.0	3.23	3.23	0.0	L
550	787.87	30.00	31.75	5.8	3.07	2.21	28.0	L
600	750.99	62.00	72.33	16.7	2.94	2.19	25.5	L

[a] The percentage deviations in the pressures and isochoric heat capacities δP and δC_V are also included.

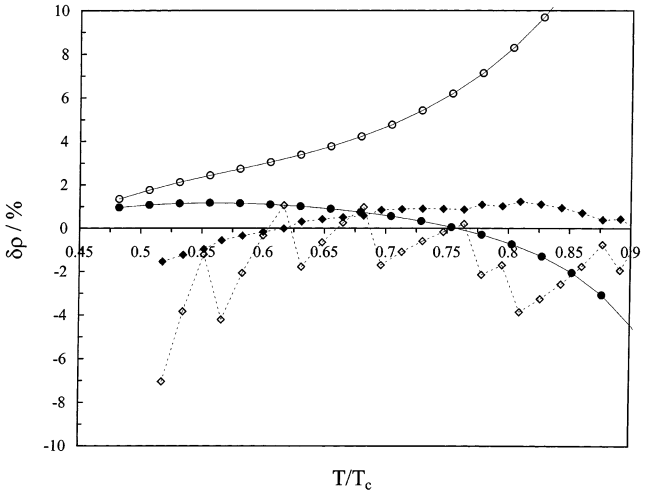

Figure 6. Percentage deviations in the saturated densities $\delta\rho^V$ and $\delta\rho^L$ of the theoretical predictions from the experimental data for ammonia. The open circles denote the vapor density deviations, and the full circles are the liquid density deviations of the DSWTEOS equation. The open diamonds denote the vapor density deviations, and the full diamonds are the liquid density deviations of the SAFT-DY equation. Interpolation lines are included just to guide the eye.

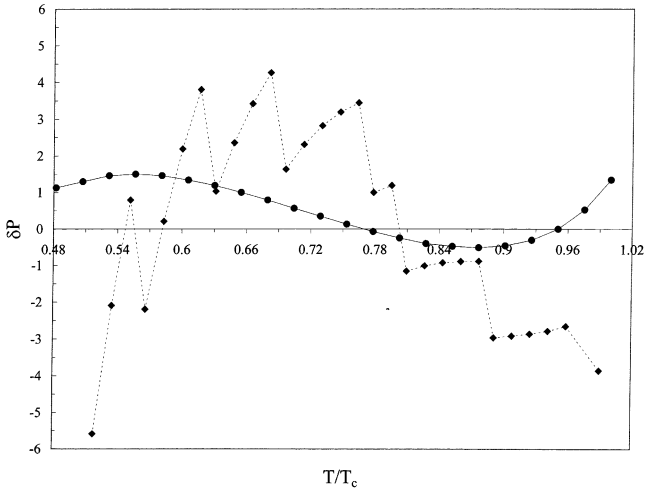

Figure 7. Percentage deviations in the saturated pressures δP of the theoretical predictions from the experimental data for ammonia. Full circles show the DSWTEOS predictions, and full diamonds, the SAFT-DY predictions. Interpolation lines are included just to guide the eye.

atures and densities. The percentage deviations δP and δC_V are also included**.** As can be seen, the predictions for these properties in the vapor and supercritical phases are good. The average of the absolute values of δP is 1.7% for the vapor phase, 6.0% for the supercritical phases, and 8.5% for the liquid phase. For the vapor and supercritical isochoric heat capacities, the average deviations are around 8%, and for the liquid phase, the average deviation is 12.1%.

4. Conclusions

In this paper we have presented the use of a perturbation theory for dipolar fluids to study polar associating substances. Despite the fact that the theory used does not model the H-bonding effects that are present in these substances, we have shown that, by using a higher value of the dipolar moment strength, it is possible to reproduce the phase diagram and other thermodynamic properties, within the same accuracy obtained by associating fluid approaches derived from the Wertheim perturbation theory. The equation of state obtained from the MSWPT (DSWTEOS) requires four parameters to be specified. This equation also predicts reasonably well the pressures and isochoric heat capacities in single phases, for water (vapor and supercritical) and ammonia (vapor, supercritical, and liquid). A complete and satisfactory prediction of the thermodynamic properties of water requires a more detailed study. We conclude in this work that the dipolar square-well fluid is a good effective intermolecular potential for water and ammonia, can be incorporated easily within a Wertheim perturbation approach to include specifically the H-bonding contribution, and can also be useful in molecular simulation studies as a primitive model in the way of finding a better realistic potential for these substances.

Acknowledgment. We are grateful to Dr. Nezbeda, Dr. Yi-Gui Li, and Dr. Gil-Villegas for providing us their data presented in this work. We appreciate helpful discussions with Dr. Gil-Villegas and the work of Miriam Zachs in improving the presentation of this article. This research was supported by CONACyT (Grant No. 41678-F).

TABLE 6: Experimental and Theoretical Pressures and Isochoric Heat Capacities for Ammonia in the Vapor (V), Liquid (L), and Supercritical (Sc) Phases[a]

T/K	ρ/(kg/m^3)	P/MPa	P^{DSWTEOS}/MPa	δP/%	C_V^{exp}/(kJ/(kg K))	C_V^{DSWTEOS}/(kJ/(kg K))	δC_V/%	phase
300	3.61	0.5	0.51	−2.3	1.82	1.63	10.4	V
325	6.84	1	1.03	−2.9	1.92	1.69	12.2	V
350	6.22	1	1.02	−2.0	1.86	1.72	7.8	V
360	2.92	0.5	0.5	0.0	1.77	1.71	3.4	V
375	5.7174	1	1.01	−1.4	1.85	1.75	5.4	V
550	66.51	15	15.84	−5.6	2.37	2.18	8.1	Sc
600	102.77	25	26.77	−7.1	2.5	2.30	8.2	Sc
650	77.469	22	23.18	−5.4	2.53	2.33	7.8	Sc
675	116.81	34	36.50	−7.4	2.63	2.41	8.3	Sc
700	62.743	20	20.86	−4.3	2.59	2.39	7.8	Sc
350	539.14	18	15.10	16.1	2.72	2.37	12.8	L
360	550.52	38	40.19	−5.8	2.71	2.37	12.6	L
375	515.92	30	27.98	6.7	2.7	2.38	12.0	L
380	510.96	32	30.16	5.8	2.69	2.38	11.5	L
385	500.55	31	28.42	8.3	2.69	2.38	11.5	L

[a] The percentage deviations in the pressures and in the isochoric heat capacities δP and δC_V are also included.

Appendix

The reduced Helmholtz free energy of the DSWTEOS can be expressed as

$$a_{\mathrm{DSW}}(T^*,\rho^*,\lambda,\mu^*) = a_{\mathrm{SW}}(T^*,\rho^*,\lambda) + a_{\mathrm{D}}(T^*,\rho^*,\mu^*) \quad \text{(A1)}$$

with the square-well term a_{SW} given as[28]

$$a_{\mathrm{SW}} = a_{\mathrm{ID}} + a_{\mathrm{HS}} + a_1/T^* + a_2/T^{*2} + a_{\mathrm{R}} \quad \text{(A2)}$$

and a Padé expression for the dipolar term given as[29]

$$a_{\mathrm{D}} = \frac{a_2^{\mathrm{D}}}{T^{*2}}\left(1 - \frac{a_3^{\mathrm{D}}}{T^* a_2^{\mathrm{D}}}\right)^{-1} \quad \text{(A3)}$$

The first term of eq A2, a_{ID}, corresponds to the ideal gas contribution to the Helmholtz free energy. For water and ammonia, we used the expression for the ideal gas free energy for a nonlinear polyatomic substance, given by McQuarrie.[36]

The second term, a_{HS}, is the Carnahan−Starling reduced Helmholtz free energy for a hard-sphere reference fluid,

$$a_{\mathrm{HS}} = \eta(4 - 3\eta)/(1 - \eta)^2 \quad \text{(A4)}$$

where $\eta = (\pi/6)\rho^*$ is the reduced packing fraction. The third term of eq A2 represents the first-order square-well perturbation term, which is given by

$$a_1 = -4\eta(\lambda^3 - 1)\exp(\mu_0 + \mu_1\xi + \mu_2\xi^2 + \mu_3\xi^3) \quad \text{(A5)}$$

where the μ_i and ξ functions are expressed as follows: and

$$\mu_0 = -\ln(1 - \eta) + (42\eta - 39\eta^2 + 9\eta^3 - 2\eta^4)/(6(1 - \eta)^3) \quad \text{(A6)}$$

$$\mu_1 = (\eta^4 + 6\eta^2 - 12\eta)/(2(1 - \eta)^3) \quad \text{(A7)}$$

$$\mu_2 = -3\eta^2/(8(1 - \eta)^2) \quad \text{(A8)}$$

$$\mu_3 = (-\eta^4 + 3\eta^2 + 3\eta)/(6(1 - \eta)^3) \quad \text{(A9)}$$

TABLE 7: Coefficients Used in the Expression for DSWTEOS

	$i = 0$	$i = 1$	$i = 2$	$i = 3$	$i = 4$	$i = 5$
ξ_{0i}	0.773853	−0.157937	0.499370	−0.115220		
ξ_{1i}	−5.58961	2.04530				
ξ_{2i}	1.216473	−2.034727	1.238574	−0.425229		
α_{1i}	187.1418	−335.6845	185.8528	−34.8731		
α_{2i}	1833.196	−5284.990	5488.597	−2453.347	402.468	
α_{3i}	−6185.698	16431.21	−16084.08	6886.400	−1091.004	
q_i	4.94876	0.097245	−12.9126	7.8632		
a_i	4.1888	2.8287	0.8331	0.0317	0.0858	−0.0846
b_i	16.4493	19.8096	7.4085	−1.0792	−0.9901	−1.0249

$$\xi = \sum_{i=0}^{2} \xi_i \eta^i \quad \text{(A10)}$$

$$\xi_0 = \sum_{i=0}^{3} \xi_{0i} \lambda^i \quad \text{(A11)}$$

$$\xi_1 = (6/\pi)(2 - \lambda)\mathrm{e}^{\xi_{10} + \xi_{11}\lambda} \quad \text{(A12)}$$

$$\xi_2 = \sum_{i=0}^{3} \xi_{2i} \lambda^i \quad \text{(A13)}$$

The coefficients ξ_{ni} in eqs A10−A13 are given in Table 7. The fourth term of eq A2 is the second-order square-well perturbation term, which is expressed as

$$a_2 = -\eta(\lambda^3 - 1)(2K_{\mathrm{HS}}^2 - (\eta\Omega(\lambda)/(1 - \eta)^3)\mathrm{e}^{(\alpha_1\eta + \alpha_2\eta^2 + \alpha_3\eta^3)}) \quad \text{(A14)}$$

with

$$K_{\mathrm{HS}} = (1 - \eta)^4/(1 + 8\eta - 2\eta^2) \quad \text{(A15)}$$

and

$$\Omega(\lambda) = (-5\lambda^5 - 5\lambda^4 + 85\lambda^3 - 75\lambda^2 - 111\lambda - 111)/(2(\lambda^2 + \lambda + 1)) \quad \text{(A16)}$$

In eq A14, the α_n are polynomials in λ whose coefficients α_{ni} are also given in Table 7. The last term of eq A2 is the residual square-well term:

$$a_{\mathrm{R}} = -\eta(\lambda^3 - 1)[4\{1 - 1.5s(\lambda)\eta\}K_{\mathrm{HS}}^2 w(\beta) + q(\lambda)\eta K_{\mathrm{HS}}^3(t^3 - \beta^3)] \quad \text{(A17)}$$

with $\beta = (1/T^*)$ and where the functions $s(\lambda)$, $q(\lambda)$, t, and $w(\beta)$ are

$$s(\lambda) = (-49\lambda^5 - 49\lambda^4 + 293\lambda^3 + 5\lambda^2 - 211\lambda - 211)/(6(\lambda^2 + \lambda + 1)) \quad \text{(A18)}$$

$$q(\lambda) = \sum_{i=0}^{3} q_i \lambda^i \quad \text{(A19)}$$

$$t = e^{\beta} - 1 \quad \text{(A20)}$$

$$w(\beta) = t - \beta - {}^1/_2\beta^2 \quad \text{(A21)}$$

The coefficients q_i of eq A19 are given in Table 7.

The terms a_2^D and a_3^D in the Padé expression (eq A3) are the second- and third-order polar perturbation terms. These terms can be expressed as fifth-order polynomials in density:

$$a_2^D = (-{}^1/_6)(\rho^*\mu^{*4})\sum_{i=0}^{5} a_i \rho^{*i} \quad \text{(A22)}$$

$$a_3^D = ({}^1/_{54})(\rho^{*2}\mu^{*6})\sum_{i=0}^{5} b_i \rho^{*i} \quad \text{(A23)}$$

The coefficients a_i and b_i of eqs A22 and A23 are given in Table 7.

References and Notes

(1) Ball, P. *Life's matrix: a biography of water*; University of California Press: 2001.

(2) Jorgensen, W. L.; Chandrasekhar, J.; Madura, J. D. R.; Impey, W.; Klein, M. L. *J. Chem. Phys.* **1983**, *79*, 926.

(3) De Pablo, J. J.; Prausnitz, J. M. *Fluid Phase Equilib.* **1989**, *53*, 177.

(4) Chapman, W. G.; Gubbins, K. E.; Jackson, G.; Radosz, M. *Int. Eng. Chem. Res.* **1990**, *29*, 1709.

(5) Guissani, Y.; Guillot, B. *J. Chem. Phys.* **1993**, *98*, 8221.

(6) Báez, L.; Clancy, P. *J. Chem. Phys.* **1994**, *101*, (11), 9837−9840.

(7) Billeter, S.; King, P.; van Gunsteren, W. *J. Chem. Phys.* **1994**, *100*, (9), 6692.

(8) Alejandre, J.; Tildesley, D. J.; Chapela, G. *J. Chem. Phys.* **1995**, *102* (11), 4574.

(9) Chialvo, A. A.; Cummings, P. T. *J. Chem. Phys.* **1996**, *105*, 8274.

(10) Galindo, A.; Whitehead, P. J.; Jackson, G.; Burgess, A. N. *J. Phys. Chem.* **1997**, *101*, 2082.

(11) Yoshii, N.; Yoshie, H.; Miura, S.; Okasaki, S. *J. Chem. Phys.* **1998**, *109* (12), 4873-4884.

(12) Kiyohara, K.; Gubbins, K. E.; Panagiotopoulos, A. Z. *Mol. Phys.* **1998**, *94* (5), 803.

(13) Mackie, A.; Hernández-Cobos, J.; Vega, L. *J. Chem. Phys.* **1999**, *111* (5), 2103.

(14) Svishchev I.; Hayward, T. *J. Chem. Phys.* **1999**, *111* (19), 9034.

(15) Mahoney, M.; Jorgensen, W. *J. Chem. Phys.* **2000**, *112* (20), 8910-8922.

(16) Kolafa, J.; Nezbeda, I. *Mol. Phys.* **2000**, *98* (19), 1505.

(17) Guillot, B.; Guissani, Y. *J. Chem. Phys.* **2001**, *115* (15), 6720-6733.

(18) Benavides, A. L.; Guevara, Y.; Del Río, F. *Physica A* **1994**, *202*, 420−437.

(19) Guevara, Y.; Benavides, A. L.; Del Río, F. *Mol. Phys.* **1996**, *89*, 1277−1290.

(20) Benavides, A. L.; Guevara, Y.; Estrada-Alexanders, A. F. *J. Chem. Thermodyn.* **2000**, *32*, 945.

(21) Guevara, Y.; Benavides, A. L.; Estrada-Alexanders, A. F.; Romero, M. *J. Phys. Chem.* **2000**, *104*, 7490.

(22) Gil-Villegas, A.; Galindo, A.; Whitehead, P. J.; Mills, S. J.; Jackson, G.; Burgess, A. N. *J. Chem. Phys.* **1997**, *106*, 4168. Galindo, A.; Gil-Villegas, A.; Jackson, G.; Burgess, A. N. *J. Phys. Chem. B* **1999**, *103*, 10272.

(23) Liu, Z.; Li, Y.; Chan, K. *Ind. Eng. Chem. Res.* **2001**, *40*, 973.

(24) Nezbeda, I.; Weingerl, U. *Mol. Phys.* **2001**, *99* (18), 1595−1606.

(25) Gil-Villegas, A. Tesis de Doctorado, Universidad Autónoma Metropolitana, México, 1993.

(26) Fleming, P. D.; Brugman, R. J. *AIChE J.* **1987**, *33*, 729.

(27) Chang, J.; Sandler, S. I. *Mol. Phys.* **1994**, *81*, 745.

(28) Fu, Y. H.; Sandler, S. I. *Ind. Eng. Chem. Res.* **1995**, *34*, 1897.

(29) Gil-Villegas, A.; Del Río, F.; Benavides, A. L. *Fluid Phase Equilib.* **1996**, *119*, 97.

(30) Larsen, B.; Rasaiah, J. C.; Stell, G. *Mol. Phys.* **1997**, *33*, 987.

(31) Landau, L. D.; Lifshitz, E. M. *Statistical Physics*, 3rd ed.; Pergamon Press: 1980; Part 1.

(32) NIST Chemistry WebBook tables, http://webbook.nist.gov/chemistry/fluid.

(33) Gray, C. G.; Gubbins, K. E. *Theory of Molecular Fluids*; Clarendon Press: Oxford, 1984.

(34) Wagner, W.; Krus, A. *Properties of Water and Steam: The Industrial Standard IAPWS-IF97*; Springer-Verlag: Berlin, 1998.

(35) Franzese, G.; Malescio, G.; Skibinsky, A.; Buldyrev, S. B.; Stanley, H. E. *Nature* **2001**, *409*, 692.

(36) McQuarrie, D. A. *Statistical Mechanics*; Harper & Row: New York, 1976.